Title

Control of exploration, motor coordination and amphetamine sensitization by cannabinoid CB1 receptors expressed in medium spiny neurons

Journal

European Journal of Neuroscience, 54(3)

ISSN

0953-816X

Authors

Bonm, Alipi V
Elezgarai, Izaskun
Gremel, Christina M
et al.

Publication Date

2021-08-01

DOI

10.1111/ejn.15381

Peer reviewed

HHS Public Access

Author manuscript

Eur J Neurosci. Author manuscript; available in PMC 2022 August 15.

Published in final edited form as:

Eur J Neurosci. 2021 August ; 54(3): 4934–4952. doi:10.1111/ejn.15381.

Control of exploration, motor coordination and amphetamine sensitization by cannabinoid CB_1 receptors expressed in medium spiny neurons.

Alipi V. Bonm[1], **Izaskun Elezgarai**[2,3], **Christina M. Gremel**[4], **Katie Viray**[1], **Nigel S. Bamford**[5,6], **Richard D. Palmiter**[7], **Pedro Grandes**[2,3], **David M. Lovinger**[4], **Nephi Stella**[1,8,*]

[1]Department of Pharmacology, University of Washington School of Medicine, Seattle, WA 98195, USA

[2]Achucarro Basque Center for Neuroscience, Science Park of the University of the Basque Country UPV/EHU, Leioa, Spain

[3]Department of Neurosciences, Faculty of Medicine and Nursing, University of the Basque Country UPV/EHU, Leioa, Spain

[4]Laboratory for Integrative Neuroscience, National Institute on Alcohol Abuse and Alcoholism, National, Institutes of Health, Bethesda, MD 20892, USA

[5]Department of Pediatrics, Neurology and Cellular and Molecular Physiology, Yale University, New Haven, CT 06510, USA

[6]Department of Neurology, University of Washington, Seattle, WA 98105, USA

[7]Howard Hughes Medical Institute and Department of Biochemistry, University of Washington School of Medicine, Seattle, WA 98195, USA

[8]Department of Psychiatry and Behavioral Sciences, University of Washington School of Medicine, Seattle, WA 98195, USA

Abstract

Activation of cannabinoid 1 receptors (CB_1R) modulates multiple behaviors, including exploration, motor coordination and response to psychostimulants. It is known that CB_1R expressed by either excitatory or inhibitory neurons mediates different behavioral responses to CB_1R activation, yet the involvement of CB_1R expressed by medium spiny neurons (MSNs), the neuronal subpopulation that expresses the highest level of CB_1R in the CNS, remains unknown. We report a new genetically modified mouse line that expresses functional CB_1R in MSN on a CB_1R knockout (KO) background ($CB_1R_{(MSN)}$ mice). The absence of cannabimimetic responses measured in CB_1R KO mice was not rescued in $CB_1R_{(MSN)}$ mice, nor was decreased spontaneous locomotion, impaired instrumental behavior, or reduced amphetamine-triggered hyperlocomotion measured in CB_1R KO mice. Significantly, reduced novel environment exploration of an open

*Author for Correspondence: Dr. Nephi Stella, Address: Health Sciences Center F404A, 1959 NE Pacific Str., Seattle, WA 98195-7280, Phone: 206-221-5220, Fax: 206-543-9520, nstella@uw.edu.

Author's contribution: A.V.B., K.V. and I.E., performed the experiments and analyzed the data. C.M.G., N.S.B., R.D.P., P.G. and D.M.L., provided tools and wrote the manuscript. N.S. designed the experiments, analyzed the data, and wrote the manuscript

field and absence of amphetamine sensitization (AS) measured in CB_1R KO mice were fully rescued in $CB_1R_{(MSN)}$ mice. Impaired motor coordination in CB_1R-KO mice measured on the Rotarod was partially rescued in $CB_1R_{(MSN)}$ mice. Thus, CB_1R expressed by MSN control exploration, motor coordination, and AS, demonstrating new functional roles for cell specific CB_1R expression at the systems level and their causal link in the control of specific behaviors.

Introduction

Multiple behaviors are controlled by endocannabinoid (eCB) signaling and influenced by phyto-cannabinoids such as Δ^9-tetrahydocannabinol (THC), the principal psychoactive ingredient of the *Cannabis* plant. Increased eCB production and treatments with THC or synthetic cannabinoids activate CB_1Rs expressed by different neuronal subpopulations that fine-tune excitatory and inhibitory neurotransmission, and regulate neuronal function, metabolism and phenotype (Busquets-Garcia et al., 2018; Lutz, 2020). In the striatum, distinct neuronal subpopulations express CB_1R at different levels: higher levels by GABAergic MSNs and parvalbumin (PV)-expressing interneurons (Uchigashima et al., 2007) and lower levels by cortical neurons that project to the striatum (Bamford et al., 2018; Glass et al., 1997; Kano et al., 2009; Tsou et al., 1998; Wang et al., 2012). Specifically, immunohistology studies show that CB_1R are expressed at high levels on MSN axon terminals that project to the substantia nigra reticulata (SNr, i.e., direct pathway) and globus pallidus (GP, i.e., indirect pathway), as well as on MSN collaterals projecting within the striatum (Davis et al., 2018; Hohmann and Herkenham, 2000; Hu and Mackie, 2015). Slice electrophysiological studies of the ventral and dorsal striatum show that cannabinoids dampen corticostriatal activity through CB_1R and CB_1R/D2 receptor heteromers located on cortical axon terminals abutting D2 receptor-expressing MSNs (Bamford et al., 2004; Marcellino et al., 2008; Pickel et al., 2006; Uchigashima et al., 2007; Wang et al., 2012; Yin and Lovinger, 2006). While promoting a minor tonic inhibition of these indirect-pathway MSNs, D2 receptor activation paired with strong post-synaptic depolarization resulting from high-frequency corticostriatal activity is sufficient to activate postsynaptic metabotropic glutamate receptors and promote long-term depression (Kreitzer and Malenka, 2005; Wang et al., 2012). In this way, CB_1R-mediated presynaptic regulation of the release of glutamate reduces signaling along the indirect pathway and participates in determining the salience of sensory input that define the reinforcing properties associated with rewarding behavior and attention (Bamford et al., 2018; Pennartz et al., 1994). Slice electrophysiology results showed that CB_1R activation reduces GABAergic inhibitory postsynaptic currents in MSN through inhibition of GABA release from terminals of recurrent axons of the MSNs themselves without direct effects on somatic ion channels (Hoffman and Lupica, 2001; Szabo et al., 1998). Accordingly, the plasticity of specific striatal microcircuits is controlled by presynaptic CB_1R expressed by GABAergic interneurons and postsynaptic CB_1R expressed by MSNs in a voltage-dependent manner that recruits eCBs and leads to a powerful disinhibition of direct pathway MSNs (Freiman et al., 2006; Mathur et al., 2013). Together, this evidence suggests a prominent role for CB_1R expressed by MSNs in the control of locomotor behavior.

Treating rodents with cannabinoid agonists triggers characteristic cannabimimetic behaviors, including four hallmark responses referred to as the “tetrad response”: hypothermia, hypolocomotion, analgesia, and catalepsy (Metna-Laurent et al., 2017; Wiley and Martin, 2003). Several studies with genetically modified mouse lines harboring cell-type specific conditional deletion of *Cnr1,* the gene encoding CB_1R*,* identified several types of neurons expressing CB_1R that are “necessary” for such cannabimimetic tetrad responses and for common locomotor and cognitive behaviors studied in mice (Bellocchio et al., 2010; Han et al., 2017; Häring et al., 2011; Lafenetre et al., 2009; Monory et al., 2007; Soria-Gomez et al., 2021; Turner et al., 2021). By contrast, few studies used genetic approaches to generate mouse lines with cell-specific conditional “rescue” of CB_1R expression to identify the CB_1R-expressing cell subpopulation that is “sufficient” for mouse behaviors and for cannabimimetic responses. Specifically, rescue of CB_1R expression in dorsal telencephalic glutamatergic neurons is sufficient to mediate social exploration and memory, as well as cannabinoid-induced hypothermia (De Giacomo et al., 2020a, b; Ruehle et al., 2013). CB_1R expressed in dorsal telencephalic glutamatergic neurons are partially sufficient for anxiety-like behaviors and for cannabinoid-induced hypolocomotion, and do not mediate cannabinoid triggered analgesia and catalepsy (De Giacomo et al., 2020a, b; Ruehle et al., 2013). Rescue of CB_1R expression in forebrain GABAergic neurons is sufficient to restore normal anxiety-like behavior and partially restores extinction of learned fear measured in CB_1R KO mice, but is not sufficient to mediate the cannabinoid induced tetrad response (De Giacomo et al., 2020b; Remmers et al., 2017). In fact, restoring CB_1R expression in forebrain GABAergic neurons on a CB_1R KO background switches the THC’s response to an increase in locomotion, revealing a cannabinoid-dependent behavior that might be occluded in wild-type (WT) and KO mouse lines (De Giacomo et al., 2020b; Remmers et al., 2017). This body of work has outlined key functional roles for cell specific CB_1R expression at the systems level and their causal link in the control of locomotor and cognitive behaviors studied in mice.

To date, no study has leveraged genetic approaches that enable a conditional “rescue” of CB_1R expression in MSN while maintaining a CB_1R KO background to test if this receptor population is “sufficient” to control these locomotor behaviors and cannabimimetic responses. Here we used a previously developed conditional flox-stop CB_1R knock-in mouse line (Naydenov et al., 2014), and backcrossed it to both the CB_1R KO mouse line (Marsicano et al., 2002) and the *Gpr88*$^{+/Cre}$ mouse line (Massart et al., 2009; Quintana et al., 2012), generating a CB_1R KO mouse line in which the *Cnr1* gene is selectively expressed only by MSNs that express Gpr88 (referred to as $CB_1R_{(MSN)}$ mice). We first validated the cell-specific expression and functionality of CB_1R in $CB_1R_{(MSN)}$ mice and studied whether $CB_1R_{(MSN)}$ mice exhibit cannabinoid-triggered tetrad responses. We also studied whether $CB_1R_{(MSN)}$ mice exhibit normal exploration and spontaneous locomotion in both a home cage and an open field, motor coordination on a Rotarod, habit formation measured in a paradigm of random interval (RI) schedules of reinforcement, and amphetamine-triggered hyperlocomotion and AS measured in an open field.

Material and methods

Mice:

All animal procedures were approved by the University of Washington Institutional Animal Care and Use Committee. Generation of *Rosa26*$^{+/fs\text{-}Cnr1}$ (Naydenov et al., 2014), and *Gpr88*$^{+/Cre}$ mice (Quintana et al., 2012), has been previously described. Animals were on a mixed C57Bl/6 and CBA (50:50) background. FsCB$_1$ mice (Naydenov et al., 2014), and *Gpr88*$^{+/Cre}$ mice were backcrossed with *Cnr1*$^{-/-}$ mice to generate *Cnr1*$^{-/-}$; *Rosa26*$^{+/fs\text{-}Cnr1}$ females and *Cnr1*$^{-/-}$; *Gpr88*$^{+/Cre}$ males, which were bred to generate CB$_1$R$_{(MSN)}$ mice and CB$_1$R KO littermate controls. WT mice were not littermate controls. Genotyping was performed using the following primers (5'>3': *Cnr1*-forward GCTGTCTCTGGTCCTCTTAAA, Cnr1-reverse GGTGTCACCTCTGAAAACAGA, *Cnr1*-neo CCTACCCGGTAGAATTAGCTT.

Immunohistochemistry:

Mice were perfused with 20 mL sterile PBS, followed by 10 mL 4% paraformaldehyde. Brains were extracted, post-fixed overnight at 4°C in 4% paraformaldehyde, then successively dehydrated in 15% sucrose and 30% sucrose for 24 h each, and finally frozen. Coronal sections were cut on a freezing microtome to a thickness of 30 μm, placed in cryoprotectant and stored at −20°C. On the day of staining, slices were removed from cryoprotectant, washed 3x in PBS, and then incubated in blocking buffer (1% Triton X-100, 5% donkey serum in PBS) for 90-min at room temperature, and then transferred to primary staining solution (0.5% Triton X-100, 2.5% donkey serum in PBS) for 72 h at 4°C. Primary antibodies and dilutions used: CB$_1$R (guinea pig, 1:2000, gift from Ken Mackie); all other primary antibodies are in Supplementary Table S1 and were optimized by performing a dilution curve paired with quantitative analysis, and dilutions in the linear phase were chosen for further staining. After primary staining, sections were washed 8x in PBS-T for 5 min. Secondary staining was performed in 0.5% Triton X-100, 2.5% donkey serum in PBS, using Alexa secondary antibodies at a dilution of 1:500 as described (Naydenov et al., 2014). After secondary staining, sections were washed 6x in PBS-T for 10 min, once in PBS, and then mounted with Fluoromount (Sigma, St Louis, MO) and sealed with nail polish.

Image collection and analysis:

Images were collected on a Leica SL confocal microscope as described (Naydenov et al., 2014). Images were analyzed and quantified in ImageJ (National Institutes of Health), using custom written macros which were applied blindly to each batch of images, and analyzed as previously reported (Horne et al., 2013).

Electron microscopy:

Mice were transcardially perfused at room temperature (20-25°C) with sterile PBS for 20 sec, followed by infusion of a fixative solution (4% formaldehyde freshly depolymerized from paraformaldehyde and 0.1% glutaraldehyde) for 10–15 min. Brains were then removed from the skull and immersion fixed in the same fixative. Coronal 50 μm striatal

vibrosections were processed for the pre-embedding immunogold method, as described (Bonilla-Del Río et al., 2019; Puente et al., 2019). Sections were preincubated in a blocking solution of 10% bovine serum albumin, 0.1 % sodium azide and 0.02 % saponin prepared in Tris–HCl buffered saline (TBS 1x, pH 7.4) for 30 min at RT. Then, they were incubated with the primary goat CB_1R antibody (2 μg/ml goat anti-CB_1R, Frontier Science Co., Japan) prepared in 0.004 % saponin concentrated blocking solution, for 48 h at 4°C. After several washes, tissue sections were incubated with 1.4-nm gold-labeled rabbit anti-goat Fab´ (1:100, Nanoprobes, Inc., Yaphank, NY) prepared in the same solution as the primary antibody for 3 h at RT. They were washed overnight at 4°C and postfixed in 1 % glutaraldehyde for 10 min. After several washes with double-distilled water, gold particles were silver-intensified with a HQ Silver Kit (Nanoprobes, Inc., Yaphank, NY) for 12 min in the dark. Then, tissue was osmicated, dehydrated and embedded in Epon resin 812. Finally, ultrathin sections were collected on mesh nickel grids, stained with lead citrate and examined in a PHILIPS EM208S electron microscope. Tissue preparations were photographed using a digital camera coupled to the electron microscope. Figure compositions were made at 600 dots per inch (dpi). Labeling, coloring and minor adjustments in contrast and brightness were made using Adobe Photoshop (San Jose, CA).

[^{35}S]GTPγS Binding Assay:

These studies were performed as previously described (Naydenov et al, in press). SNr tissue was dissected on ice and homogenized in ice-cold Homogenization buffer (50 mM Tris-HCl pH 7.4, 3 mM $MgCl_2$, and 1 mM EGTA). The homogenate was centrifuged at 45,000 x g for 10 min at 4°C, and then the pellet was homogenized in 50 mM Tris-HCl, with 3 mM $MgCl_2$, 1 mM EGTA and 100 mM NaCl. Membrane homogenates were incubated with 3 mU/ml adenosine deaminase (Roche Applied Science, IN) in Homogenization buffer for 10 min at 30°C, to inactivate endogenous adenosine. Afterwards, 10 μg of protein per reaction was incubated in Reaction buffer (0.1% BSA, 30 μM GDP, 0.1 nM [^{35}S]GTPγS, Perkin Elmer, OH) and 0.6 mU/ml adenosine deaminase, with either 140 μM CP55,940 or vehicle, for 45 min at 30°C. The incubation was terminated by vacuum filtration through Whatman filters (GE Healthcare), followed by three washes with 3 ml ice-cold Tris-HCl, pH 7.4. Bound [^{35}S]GTPγS was quantified using a liquid scintillation counter in vials containing isolated [^{35}S]GTPγS-bound filter paper along with 4ml of Ecoscint scintillation fluid (National Diagnostics).

Cannabinoid Tetrad:

Core body temperature was determined by rectal probe. Catalepsy was measured by placing the forelimbs on a horizontal bar raised 3 cm above the bench and recording the latency for the mouse to either remove its forepaws from the bar or climb up onto the bar. For each mouse, a total of three attempts were made, and if a mouse fell off the bar or moved during forepaw placement then the trial was recorded as 0 sec. The maximum latency of the three trials was recorded as the final measure. Tail flick analgesia was measured by submersing the tip of the mouse's tail in a 56 C° ± 2 C° water bath and recording latency to withdrawal (immediate withdrawal was recorded as 0 sec). Locomotion was measured in an open field chamber (cm: 25×45×45) with a vertically mounted camera, and the movement of each mouse was tracked in Ethovision (Wageningen, the Netherlands).

Phenotyper home-cage monitoring system:

Male mice were singly housed in Noldus Phenotyper chambers (Wageningen, the Netherlands) for 72 h. Behavior was monitored by a vertically mounted camera and analyzed in Noldus Ethovision. Mice had *ad libitum* access to food and water, and testing was performed in a sound-attenuated room with a 12 h light/dark cycle. With the exception of novelty locomotion, which was recorded during the initial two hours of housing in the Phenotyper chambers, measures of spontaneous locomotion during light and dark cycle were taken during 48 h (beginning at 24 h and ending at 72 h after housing in the Phenotyper chambers).

Rotarod:

Mice were given one 5 min training session prior to Rotarod (Columbus Instruments, OH) testing, with the rotational speed set at a constant 4 rpm. On the second day, seven consecutive trials were run, without an initial training session. Mice were then rested in their home cage for 30 min between sessions, and then were returned to the Rotarod for seven consecutive trials during which the Rotarod accelerated from 4 to 40 rpm at a rate of 0.2 rpm / 40 s, and latency to fall was recorded. Mice were rested for 30 min between trials in their home cages. Each lane was cleaned with 70% ethanol between trials.

Instrumental behavior:

Mice were food restricted to 80-90% of starting body weight, were fed daily after each behavioral session, and continuous access to water in home cage. Behavioral training and testing were performed in sound-attenuated operant chambers (Med Associates, VT). Each chamber was illuminated by a house light at the start of each testing session and remained on throughout the session and had a retractable lever that was present either on the left or right side of a central food dispenser. Reinforcers (20 mg food pellets; BioServ) were delivered from the food dispenser into the food receptacle equipped with detectors to record head entries. During the first session, mice were placed in the operant chambers for 30 min, and single reinforcers were delivered on a random time interval (60 sec) schedule (no lever was present for this first training session). For the following 4 days, animals were placed in the operant chambers for 30 min under a continuous reinforcement schedule where each lever press made was rewarded with a single reinforcer, until the mice received a max of 30 reinforcers or 1 h had passed. After the animals had learned to lever press for reinforcers, they were trained on a random interval (RI) schedule for 7 consecutive days. The first 2 days, mice were trained under a RI30 (i.e., reinforcer delivered on the first lever press after an average 30 sec had passed from the previous earned reinforcer), followed by 5 days of RI60. The session would end with lever retraction and turning off the house light after 30 reinforcers were earned or 60 min had passed. Each day, post-training mice were given access to a 20% sucrose solution in their home cage. Devaluation testing was conducted across 2 days (Valued Day, and Devalued Day) and began 24 h after the last training day. Mice were given *ad libitum* access to either the earned reinforcer (food pellets) on the Devalued Day or a 20% sucrose solution on the Valued day for 1 h prior to testing. Immediately following the *ad libitum* access on each day, mice were placed in the operant chambers for 5 min and number of lever presses were recorded, but no

reinforcers were delivered. Assigned lever (left or right) and devaluation day (Valued and Devalued) order were counterbalanced across groups. Devaluation index was calculated as (presses valued condition - presses devalued condition) / (presses valued condition + presses devalued condition).

Amphetamine treatment and sensitization monitored in an open-field chamber:

A two-injection protocol of sensitization was used, as described in (Corbillé et al., 2007). Group-housed male mice were habituated to the behavioral chamber for 90-min prior to all sessions. During the first two sessions (days 1-2), the animals received a saline injection after habituation, and were placed back in the chamber for a further 90 min. On day 3, the animals received 2 mg/kg amphetamine after habituation, and then were placed in the locomotor chambers for 90 min for locomotor measurement. The animals were rested for 6 days, and then on day 10, the animals were again habituated, and then injected with 2 mg/kg amphetamine and returned to the locomotor chamber for 90 min. Locomotor chambers were equipped with laser sensors and locomotion was recorded from beam breaks. Locomotor chambers were cleaned with Clidox (Pharmacal, CT) and supplied with fresh bedding (Bed-o-Cobs, Andersons Lab Bedding, OH) between trials.

Statistical analysis:

Statistical analysis was performed using GraphPad PRISM 9 (San Diego, CA, USA) and are specified for each result in either the main text or figure legends.

Results

Validation of CB_1R expression and functionality in $CB_1R_{(MSN)}$ mice.

We developed a genetic *Rosa26*$^{+/fs\text{-}Cnr1}$ construct that has Cre recombinase under the *Gpr88* regulatory elements known to be robustly expressed by both direct- and indirect-pathway MSNs (Quintana et al., 2012) (a diagram of the genetic construct is in supplementary figure S1A). Thus, breading *Cnr1*$^{-/-}$; *Gpr88*$^{+/cre}$ males with *Cnr1*$^{-/-}$; *Rosa26*$^{+/fs\text{-}Cnr1}$ females led to progenies with restricted *Cnr1* expression in MSNs and on a CB1R KO background ($CB_1R_{(MSN)}$ mice). Semi-quantitative immunohistochemistry (sqIHC) analyses of CB_1R expression in MSN terminals projecting to the SNr and GP indicated that CB_1R expression in SNr was absent in CB_1R KO mice and rescued in $CB_1R_{(MSN)}$ mice to 45±18% of WT levels (Figure 1A). Similarly, CB_1R expression in GP was absent in CB_1R KO mice and rescued in $CB_1R_{(MSN)}$ mice to 57±16% of WT CB_1R levels (Figure 1B). Thus, this genetic approach results in CB_1R expression in MSN that approximates heterozygous expression levels (Davis et al., 2018).

CB_1R functionality in MSNs was confirmed by measuring cannabinoid stimulated [S^{35}]GTPγS binding in tissue homogenates, an index of G protein activation (Steindel et al., 2013). Thus, as previously described, we tested the CB_1R agonist CP55940 at its EC_{80} dose of 140 nM (Naydenov et al., 2014) and measured [S^{35}]GTPγS binding in SNr homogenates harvested from WT, $CB_1R_{(MSN)}$ and CB_1R KO mice. Figure 1C shows that CP55940 increased [S^{35}]GTPγS binding by 148±7% in WT, by 134±3% in $CB_1R_{(MSN)}$ and

was inactive in CB_1R KO (104±11%). We conclude that $CB_1R_{(MSN)}$ mice express functional CB_1Rs on MSNs.

To confirm the cellular specificity of our genetic approach, we imaged brain sections encompassing the dorsal striatum for GFP expression as our genetic construct includes enhanced green fluorescent protein (EGFP) that is expressed from the same transcript by using the internal ribosome entry sequence (IRES) (Supplementary figure S1). Low-resolution, fluorescence imaging of coronal brain sections from $CB_1R_{(MSN)}$ mice revealed that EGFP was principally expressed in the striatum (Supplementary figure S2). Imaging of EGFP expression in brain sections co-stained with DARPP32, a marker of MSNs, showed that a large fraction of DARPP32-expressing cells expresses EGFP (Figure 1D). sqIHC analysis indicated that 90% of DARPP32-labelled neurons expressed GFP and only 10% of DARPP32-labelled neurons did not co-express EGFP (Figure 1E). EGFP was not detected in GABA interneurons expressing calretinin (Figure 1F), neuropeptide Y (Figure 1G), and parvalbumin (Figure 1H), or in choline acetyltransferase-expressing cholinergic interneurons (Figure 1I), suggesting that this genetic approach captures nearly all MSNs and none of the main striatal interneuron populations.

CB_1R expression in the striatum is greatly heterogeneous and encompasses three principal components: 1] CB_1R expressed by terminals of cortical origin, 2] CB_1R expressed by various types of interneurons and 3] CB_1R expressed by MSN-MSN co-laterals, the combination of which complicates the visualization and identification of CB_1R expression by select cellular populations (Davis et al., 2018; Freiman et al., 2006; Mathur et al., 2013; Matyas et al., 2006; Uchigashima et al., 2007). To study CB_1R expression by MSN-MSN co-laterals, we used electron microscopy (EM) to visualize rescued CB_1R expression in MSN on a CB_1R KO background. Figure 2A–B show striatal sections from WT mice with CB_1R labeling on both asymmetric synapses (i.e., glutamatergic) and symmetric synapses (GABAergic). Note that CB_1R are not found on symmetric dopamine axon boutons or cholinergic interneurons, as reviewed in Covey et al (Covey et al., 2017). CB_1R-positive inhibitory profiles were identified by pleomorphic, vesicle-containing axon terminals contacting dendrites (Figure 2A–B). Small, positive excitatory buttons containing spherical vesicles made asymmetrical contact over dendritic spines (Figure 2B). By contrast, a striatal section from a $CB_1R_{(MSN)}$ mouse showed CB_1R labeling only on symmetric synapses that occasionally contained dense-core vesicles (Figure 2C–D) as emphasized by the lack of CB_1R labeling on asymmetric synapses (Figure 2C). Importantly, no CB_1R labeling was detected in striatal sections from CB_1R KO mice, demonstrating antibody staining specificity (Figure 2E–F). These results further validate the expression of CB_1R by MSNs in the $CB_1R_{(MSN)}$ mouse line, and extend previous studies suggesting CB_1R on MSN-MSN collateral terminals within the striatum (Matyas et al., 2006; Uchigashima et al., 2007). Thus, $CB_1R_{(MSN)}$ mice express CB_1R in MSN terminals projecting to the GP and the SNr and in MSN collaterals.

Absence of cannabimimetic responses in $CB_1R_{(MSN)}$ mice.

We previously reported that global rescue of CB_1R expression in CB_1R KO mice by crossing $Cnr1^{-/-}$;$Rosa26^{+/fs\text{-}Cnr1}$ mice to $Cnr1^{-/-}$; $Gpr88^{+/cre}$ (i.e., Global-fsCB_1R mice)

results in the full rescue of the CP55940-triggered cannabimimetic tetrad response (Naydenov et al., 2014). Here we tested if $CB_1R_{(MSN)}$ mice also exhibited a cannabinoid-triggered tetrad response. As expected, CP55940 triggered the tetrad response in WT mice: 1) 7°C reduction in body temperature measured using a rectal probe (Figure 3A); 2); reduction of locomotion measured in an open field (Figure 3B), analgesia as indicated by the latency to withdraw the tail from hot water (Figure 3C), and catalepsy as measured by the latency to withdraw from a standing horizontal bar (Figure 3D). By contrast, CP55940 did not trigger the cannabimimetic tetrad response in either CB_1R KO or $CB_1R_{(MSN)}$ mice (Figure 3A–D). We conclude that functional CB_1R expression by MSN to approximately 50% of WT levels is not sufficient to restore CP55940-triggered cannabimimetic tetrad response.

Locomotor behavior of $CB_1R_{(MSN)}$ mice.

We studied whether $CB_1R_{(MSN)}$ are involved in spontaneous locomotion by using the Noldus PhenoTyper® system, an instrumented home cage that tracks mice over multiple days and allows for the detection of subtle differences in daily patterns of spontaneous locomotion and time spent in defined areas of the home cage (e.g., close to the edges and in hidden areas) (Pham et al., 2009; Steele et al., 2007). Mice of each genotype were single housed in PhenoTyper cages for 72 h and distance travelled in select areas of the home cage were measured by video recording (Figure 4A). Analysis of spontaneous locomotion during the first 2 h of being placed in the home cage (an index of increased activity linked to exploration, (Bourin and Hascoët, 2003)) indicated that both CB_1R KO and $CB_1R_{(MSN)}$ mice moved significantly less compared to WT mice (Figure 4B). Further, spontaneous locomotion during the light phase (when mice are less active) was also significantly lower for both CB_1R KO and $CB_1R_{(MSN)}$ mice compared to WT mice. (Figure 4B). Of note, all genotypes had comparable overall activity during dark phase (when mice are more active) (Figure 4B), as well as comparable time spent immobile, close to the edges of the home cage and in the hidden area of the home cage during both light and dark phases (Figure 4C–E). These results suggest that deficits in spontaneous locomotion measured in CB_1R KO mice during both initial exploration and the light phase are not rescued in $CB_1R_{(MSN)}$ mice, and that spontaneous locomotion measured during the during dark phase (active) is independent of CB_1R. Further, these results also indicate no overt differences in anxiety-like and depressive-like behaviors between mice of all genotypes as suggested by comparable time spent close to the edges and in the hidden area of the home cage.

Normal motor coordination and the acquisition of motor coordination skills requires functional MSNs and can be studied using a Rotarod apparatus by comparing the latency of mice to fall from the Rotarod over multiple trials (two days of 7 trials per day; 3 min/trial) (Costa et al., 2004). Figure 5A–B show that the overall average performance of CB_1R KO mice on the Rotarod was poor compared to WT mice on both days, and that overall average Rotarod performance of $CB_1R_{(MSN)}$ mice was comparable to WT mice on day 1, and yet comparable to CB_1R KO mice on day 2. To measure fast and slow learning of motor coordination skills, we adopted a paradigm developed by Costa et al. in which fast learning is measured as an improvement in performance during the initial trials of each day (Trial 2 – Trial 1), and slow learning is measured by the sum of improvement in performance

across the final trials of each day ([(Trial 6 – Trial 5) + (Trial 7 – Trial 6)]/2) (Costa et al., 2004). Figure 5C shows that mice of all genotypes exhibited similar fast learning on the first day of Rotarod testing, and that $CB_1R_{(MSN)}$ mice exhibited improved fast learning compared to WT and CB_1R KO mice on the second day of Rotarod testing. This result suggests that $CB_1R_{(MSN)}$ mice exhibit enhanced learning of motor coordination skills during the initial trials of the 2nd day of Rotarod testing, possibly through enhanced MSN synaptic plasticity occurring during this behavior in $CB_1R_{(MSN)}$ mice. Figure 5D shows that mice of all genotypes exhibited comparable slow learning of motor coordination on both days of Rotarod testing. These results extend previous findings showing that CB_1R contributes to both motor coordination and the acquisition of new motor coordination skills; and suggests a role for CB_1R expressed by MSN in this locomotor behavior.

$CB_1R_{(MSN)}$ is not sufficient to rescue deficit in habit formation measured in CB_1R KO mice.

Shifting between goal-directed and habitual actions allows for efficient and flexible, decision making, and involves dynamic adaptation of cortico-striatal neuronal circuits that underlie individual behavioral strategies (Balleine and O'doherty, 2010). Outcome devaluation paradigms can be used to examine goal-directed and habitual control over actions; goal-directed actions are sensitive to the current expected outcome value, while habits are not. RI schedules of reinforcement have been shown to bias development of habitual behaviors as evidenced by an insensitivity to outcome devaluation, and CB_1R KO mice fail to form such habits, showing goal-directed behavior following RI schedule training (Gremel and Costa, 2013; Peak et al., 2019). Thus, mice were initially trained for 3 days to lever press on a continuous reinforcement (CRF) schedule (with the potential to earn 5, 15, and 30 rewards), for 2 days on a RI30 schedule (reinforcement follows the first press after 30 sec on average has passed) and 4 days of RI60 (reinforcement follows the first press after 60 sec on average has passed). As expected, WT mice increased pressing rate across days of training in all schedules and exhibited the most pronounced increased in pressing rate the first training days of RI30 and RI60 schedules (Two-way ANOVA: $P<0.001$) (Figure 6A). While both CB_1R KO and $CB_1R_{(MSN)}$ mice also increased lever-pressing rates across training in all schedules and exhibited a more pronounced increase in pressing rate the first training days of RI30 and RI60 schedules (Two-way ANOVA: $P<0.001$), these mice made overall fewer lever presses during RI30 (compare to WT mice response: CB_1R KO mice = 42% and $CB_1R_{(MSN)}$ mice = 48%), and fewer level presses during RI60 schedules (compare to WT mice response: CB_1R KO mice = 61% and $CB_1R_{(MSN)}$ mice = 64%) (Figure 6A). Figure 6B shows that, as expected, WT mice made similar number of presses during valued and devalued days, indicating that they were insensitive to outcome devaluation and that their responses were habitual. Figure 6B also shows that both CB_1R KO and $CB_1R_{(MSN)}$ mice made more lever presses on valued versus devalued days, indicating their actions were goal-directed. Similar results were obtained when analyzing the rate of lever presses (i.e., press/min) during acquisition (Figure 6C) and the normalized rate of presses for the valued and devalued presses (Figure 6D). Importantly, mice of all genotypes earned similar reinforcements (Figure 6E), made similar numbers of head entries (Figure 6F), and consumed similar amounts of pellets and sucrose during devaluation procedures (Supplementary Figure S3). These results show that functional CB_1R expression by MSN to

approximately 50% of WT levels is not sufficient to rescue the loss of habitual control over actions exhibited by CB_1R KO.

$CB_1R_{(MSN)}$ rescues amphetamine sensitization without rescuing impaired amphetamine-triggered hyperlocomotion in CB_1R KO mice.

The psychostimulant amphetamine modulates neurotransmission in striatal and limbic brain areas that increases locomotion and reward-related behaviors (Bamford et al., 2018; Bamford et al., 2004; Reith and Gnegy, 2019; Wang et al., 2013). We tested whether CB_1R expression in MSNs would be sufficient to rescue the reduced amphetamine-triggered hyperlocomotion measured in CB_1R KO mice (Corbillé et al., 2007). Mice were habituated to an open-field chamber for 2 consecutive days (i.e., 90 min habituation followed by a saline i.p. injection and a further 90 min behavioral recording on both days). On the 3rd day, mice were placed in the open-field chamber for 90 min, injected with amphetamine (2 mg/kg), and locomotion was recorded for an additional 90 min. Figure 7A–B shows that both CB_1R KO and $CB_1R_{(MSN)}$ mice displayed a reduced amphetamine-triggered hyperlocomotion compared to WT mice (Two-way ANOVA: $P<0.001$). Of note, only CB_1R KO mice exhibited reduced exploratory behavior compared to WT mice when analyzing locomotion during the initial 10 min (Figure 7C), and $CB_1R_{(MSN)}$ mice exhibited increased ambulation compared to both WT and CB_1R KO mice when analyzing locomotion following exploration (10 min to 90 min, Figure 7D). These results show that CB_1R expression in MSN is not sufficient to rescue the reduced amphetamine-triggered hyperlocomotion measured in CB_1R KO mice. These results also suggest that CB_1R expression in MSN is involved in exploration and following ambulation measured in an open field.

Behavioral sensitization to amphetamine is expressed as a progressive enhancement of locomotion with repeated amphetamine injections. In mice, CB_1R are involved in the induction of AS (Corbillé et al., 2007) and can be measured by the long-lasting hypersensitivity to its stimulatory effect on locomotion (Opiol et al., 2017; Richetto et al., 2013; Vezina and Stewart, 1989). Figure 7E shows that $CB_1R_{(MSN)}$ mice displayed similar AS compared to WT, whereas CB_1R KO mice did not exhibit significant AS. These results show that functional CB_1R expression by MSN to approximately 50% of WT levels is sufficient to fully rescue the absence of AS measured in CB_1R KO.

Discussion

We report a new genetically modified mouse line, $CB_1R_{(MSN)}$ mice, that expresses functional CB_1R in MSN at approximately 50% of WT levels and on a CB_1R KO background. Studying this mouse line, we found that CB_1Rs in MSN are sufficient to rescue several impaired behaviors exhibited by CB_1R KO mice: it fully rescues novel environment exploration of an open field and AS, and partially rescues impaired motor coordination measured on the Rotarod. We also show that partial CB_1R re-expression in MSN on a CB_1R KO background is not sufficient to rescue cannabinoid-triggered tetrad and several other deficits in motor behaviors measured in CB_1R KO mice, including decreased spontaneous locomotion in a home-cage system measured during both the initial exploration period and

the light cycle, the impaired instrumental behavior measured by the shift in goal directed actions to habit formation, and hyperlocomotion triggered by amphetamine.

Genetic approach, molecular anatomy and limitations:

All molecular components that form the eCB signaling system are present in MSN (Covey et al., 2017; Uchigashima et al., 2007). Slice electrophysiology studies indicate that the two main eCBs – anandamide and 2-arachidonyl glycerol – are produced by MSN in an activity-dependent manner and serve as distinct retrograde messengers that activate presynaptic CB_1R and regulate the release of multiple neurotransmitters in the basal ganglia (Adermark et al., 2009; Covey et al., 2017). Thus, eCB produced by MSNs bind to nearby CB_1R on terminals of cortico-striatal projections, terminals of select types of striatal interneurons and terminals of MSN co-laterals, and eCB produced in the GP and SNr activate nearby CB_1R on terminals of MSN projections (Bamford et al., 2004; Marcellino et al., 2008; Pickel et al., 2006; Uchigashima et al., 2007; Wang et al., 2012; Yin and Lovinger, 2006). Our EM results extend previous studies that visualized CB_1R expression in the striatum by providing further evidence for CB_1R expression on MSN-MSN collateral terminals and confirming CB_1R labeling on both asymmetric synapses (i.e., glutamatergic) and symmetric synapses (GABAergic).

CB_1R expression on MSN-MSN collateral terminals have been implicated in mechanisms of disinhibition circuits that control locomotor behaviors and the actions of psychostimulants (Dobbs et al., 2016). Specifically, CB_1R is expressed at higher levels by D2 indirect pathway MSN collaterals in caudal dorsolateral striatum (Kreitzer and Malenka, 2005; Wang et al., 2012), which may inhibit GABA release onto direct pathway MSNs (Davis et al., 2018). Analyses of CB_1R expression in the basal ganglia indicates an anatomical gradient and suggests that these receptors participate in “gating” and integrating striatal output by inhibiting GABA release in the striatum and enhancing postsynaptic cells activation by glutamatergic and/or dopaminergic afferents (Davis et al., 2018; Wang et al., 2012).

While $CB_1R_{(MSN)}$ mice enable the testing for the sufficiency of this receptor population on a CB_1R KO background, this genetic approach has key limitations. The *Gpr88* gene is similarly expressed in direct and indirect pathway MSNs (Massart et al., 2009), and after recombination, CB_1R expression is no longer dependent upon the endogenous *Cnr1* promoter but instead depends on the CBA promoter, which is a combination of cytomegalovirus promoter and chicken β-action promoter region including an intron, to drive gene expression (Luo et al., 2002). Thus, rescue of CB_1R expression in MSN using this genetic approach does not recapitulate the endogenous dorsolateral to ventromedial gradient of CB_1R expression in the striatum, and the known difference in function of CB_1R in direct/indirect MSNs (Davis et al., 2018). For example, native CB_1R are expressed at high levels in striosomes in the dorsolateral and lateral striatum, where they are enriched in MSN collaterals (Davis et al., 2018). Comparable expression of CB_1R in both the direct and indirect pathway will not restore the balance provided by the striatal expression gradient of CB_1R in basal ganglia, which could affect specific behaviors of $CB_1R_{(MSN)}$ mice. It is also important to consider the molecular mechanisms of compensation that might occur in the absence of endogenous CB_1R expression during development (Maccarrone et al.,

2014). For example, this could result in the imbalance between synaptic excitation and inhibition within the circuit caused by expression of CB_1R in MSNs only, which could result in developmental changes underlying some of our behavioral findings. Specifically, it is unclear if the enhanced fast motor learning measured on the second day of Rotarod testing and the enhanced ambulation in open field detected in $CB_1R_{(MSN)}$ mice compared to WT mice reflect a compensatory mechanism or is revealing a $CB_1R_{(MSN)}$-dependent behavior occluded in WT and KO mouse lines. We also note that use of the GPR88 mouse does not rescue of CB_1R expression in excitatory neurons and parvalbumin-positive interneurons, and thus perhaps the $CB_1R_{(MSN)}$-dependent behavior relies on such expression. Finally, this genetic approach leads to the expression of functional CB_1R that reach heterozygote levels (approximately 50% of WT levels), and no statistical difference between the cannabinoid triggered [S^{35}]GTPγS binding in CB_1R KO and $CB_1R_{(MSN)}$ brain tissues (post-hoc comparison: ANOVA followed by Tukey's multiple comparison test). This is important because it suggests that 1) only partial re-expression of CB_1R is necessary to achieve a fully, or near-fully coupled functional response, and 2) activation of only a fraction of the CB_1R reserve is necessary to observe a full physiological response in the WT mice. These data help interpret the partial (i.e., heterozygous-like expression) restoration of CB_1R levels in $CB_1R_{(MSN)}$ mice. Thus, we conclude that CB_1R functionality in MSNs might represent a rate-limiting molecular step in the context of both impaired motor coordination and reduced initial exploration of an open field (i.e., partial rescue).

Cannabinoid-triggered tetrad behaviors:

It is known that CB_1R expression in dorsal telencephalic glutamatergic neurons is sufficient to mediate cannabinoid-induced hypothermia and hypolocomotion, and do not mediate cannabinoid triggered analgesia and catalepsy; and that CB_1R expression in forebrain GABAergic neurons is not sufficient to mediate any of the cannabinoid-triggered cannabimimetic tetrad response (De Giacomo et al., 2020b; Ruehle et al., 2013). Our results show that CB_1R in MSN on a CB_1R KO background are not sufficient to mediate the cannabinoid-induced tetrad response, further strengthening the conclusion that GABAergic transmission is not involvement in the cannabinoid-triggered tetrad response.

Exploration and spontaneous locomotion:

Well-balanced exploration represent a fundamental behavior for survival and is often dysfunctional in psychiatric disorders, and is controlled by CB_1Rs (Häring et al., 2011; Newcorn, 2001; Sarris et al., 2020). To our knowledge, no study tested the involvement of CB_1R in locomotion using real-time monitoring of spontaneous locomotion in a home-cage system and over several days of light and dark cycles. We found that rescue of CB_1R in MSN on a KO background does not rescue decreased spontaneous locomotion measured in CB_1R KO mice during both the initial exploration period of the home-cage system and the light cycle, suggesting that a different neuronal type expressing CB_1R is involved in these spontaneous locomotion behaviors. Remarkably, rescue of CB_1R in MSN on a CB_1R KO background rescues the decreased spontaneous locomotion measured in CB_1R KO mice during the exploration period in an open field, a result that extends previous studies showing that CB_1R expressed in dorsal telencephalic glutamatergic neurons are sufficient to rescue such CB_1R KO behavioral impairment (De Giacomo et al., 2020a). The difference

in results between home-cage and open-field environments could be linked to differences in light intensity and novelty saliency between a more familiar environment reproduced by a home-cage system and unfamiliar environment linked to an open field and agrees with studies on the role of CB_1R in social interaction and exploration of unknown individuals (De Giacomo et al., 2020a).

Motor coordination:

To our knowledge, only one study reported the performance of CB_1R KO mice on the Rotarod apparatus by measuring their latency to fall over 3 trials/day in a 1-day testing paradigm and found no difference in performance compared to WT mice (Blazquez et al., 2011). Our results agree with this study as we also did not detect a difference between genotypes during the initial 3 trials of Rotarod on day one; and extends this study by showing that CB_1R KO mice perform significantly worse than WT mice when measuring Rotarod performance over multiple trials (two days of 7 trials per day). Considering that impaired learning of motor coordination is thought to result from dysfunction of the cortico-striatal neuronal circuits that encompasses MSNs (Walker, 2007), our results suggest that CB_1Rs expressed within the cortico-striatal neuronal circuits are involved in improving motor coordination skills.

Goal-directed and habitual actions:

Behavioral studies in both humans and rodents show that performance in decision-making tasks depends on two learning processes; one encoding the relationship between actions and their consequences, and a second involving the formation of stimulus–response associations (Yin et al., 2006). These learning processes are thought to govern goal-directed and habitual actions, respectively, and depend on homologous cortico-striatal neuronal circuits (Yin et al., 2006). CB_1Rs play a key role in the behavioral shifts between habit formations and goal-directed actions and may participate in distorted behaviors often observed in obsessive compulsive disorder and addiction (Hilário et al., 2007). These action strategies are likely encoded by different neuronal populations in corticostriatal neuronal circuits, and a shift in behavior would correspond to a shift in the activity of neuronal projections controlling goal-directed actions and habit formations. Our results show that CB_1R expression in MSN is not sufficient to rescue habit formation exhibited by CB_1R KO mice indicating that that a different neuronal type expressing CB_1R is involved in this behavior (Gremel et al., 2016).

Amphetamine hyperlocomotion and sensitization:

At low doses, amphetamine exhibits therapeutic properties, including relieving symptoms associated with attention deficit hyperactivity disorder, narcolepsy, and obesity; but repetitive use of large doses of amphetamine contributes to subjective reward and positive reinforcement and may lead to addiction, impaired cognitive function, and psychosis (Berman et al., 2009; Parsons and Hurd, 2015). Accordingly, it is important to better understand the molecular, cellular and systems mechanism of amphetamine's bioactivity to optimize its potential therapeutic applications. Amphetamine increases neurotransmission in limbic brain areas involved in locomotion and motivation by, for example, increasing dopamine release, activating D2 receptors that suppress indirect pathway MSNs and increase motor activity (Robinson and Becker, 1986; Sulzer et al., 2005). It is known that changes

in eCB signaling controls psychostimulant responses in mice. Specifically, Corbillé et al. were the first to show that CB_1R blockade during the first amphetamine treatment reduces both amphetamine-triggered hyperlocomotion and AS, whereas CB_1R blockade during the 2^{nd} amphetamine treatment does not affect the expression of AS (Corbillé et al., 2007). AS is associated with change in gene expression and remodeling of neuronal circuits in striatum, both of which are controlled by CB_1R (Corbillé et al., 2007; Jang et al., 2020). We show that CB_1R expression in MSN is not sufficient to rescue amphetamine-triggered hyperlocomotion and yet is sufficient to fully rescue the absence of AS exhibited by CB_1R KO mice. Thus, our study emphasizes a new player (CB_1R expressed by MSN) that is required and sufficient to the development of AS and suggests their involvement in reward and positive reinforcement behaviors. Considering results showing that preserved goal-directed behavior might enhance reward-driven responses, activation of CB_1R expressed by MSN might contribute to the development of addiction, impaired cognitive function, and psychosis.

In summary, we report a new genetic mouse line ($CB_1R_{(MSN)}$ mice) and discovered that CB_1R expressed by MSN play a key function in exploration, motor coordination and AS, demonstrating new functional roles of CB_1R at the systems level and their causal link in the control of select behaviors. Current cannabinoid-based treatments are often associated with side effects that limit the desired therapeutic effect. Our study might help provide the molecular and cellular understanding needed to develop therapeutics that target select MSN-dependent behaviors, for example to favor amphetamine-based therapeutic response while reducing their side-effects.

Supplementary Material

Refer to Web version on PubMed Central for supplementary material.

Funding, Disclosure and Acknowledgments:

This work was supported by the National Institutes of Health [Grants DA047626 and DA026430 to N.S., NS060803 to N.S.B., ZIAAA000416 to D.M.L. AA026077 to C.M.G.]; MINECO/FEDER, UE (Grant SAF2015-65034-R to P.G.); Ministerio de Ciencia e Innovación (Grant PID2019-107548RB-I00 to P.G.); Red de Trastornos Adictivos, Instituto de Salud Carlos III (ISC-III); European Regional Development Funds-European Union (ERDF-EU) (Grant RD16/0017/0012 to P.G.); The Basque Government (Grant IT1230-19 to P.G.). A.V.B., I.E., C.M.G., K.S., N.S.B., R.D.P., P.G. and D.M.L. reported no financial interests or potential conflicts of interest. We thank Margaret I. Davis for critical reading of the manuscript. Nephi Stella is employed by Stella Consulting LLC. The terms of this arrangement have been reviewed and approved by the University of Washington in accordance with its policies governing outside work and financial conflicts of interest in research.

Data availability statement:

All data can be obtained upon request to the corresponding author.

Abbreviations:

AS	Amphetamine sensitization
AUC	area under the curve
CB_1R	cannabinoid CB_1 receptor

CRF	continuous reinforcement
EM	electron microscopy
eCB	endocannabinoid
EGFP	enhanced green fluorescent protein
GP	globus pallidus
KO	knockout
MSN	medium spiny neuron
RI	random interval
sqIHC	semi-quantitative immunohistochemistry
SR1	SR141617
SNr	substantia nigra reticulata
THC	Δ^9-tetrahydocannabinol
WT	wildtype

References:

Adermark L, Talani G, and Lovinger DM (2009). Endocannabinoid-dependent plasticity at GABAergic and glutamatergic synapses in the striatum is regulated by synaptic activity. European Journal of Neuroscience 29, 32–41. [PubMed: 19120438]

Balleine BW, and O'doherty JP (2010). Human and rodent homologies in action control: corticostriatal determinants of goal-directed and habitual action. Neuropsychopharmacology 35, 48–69. [PubMed: 19776734]

Bamford NS, Wightman RM, and Sulzer D (2018). Dopamine's Effects on Corticostriatal Synapses during Reward-Based Behaviors. Neuron 97, 494–510. [PubMed: 29420932]

Bamford NS, Zhang H, Schmitz Y, Wu NP, Cepeda C, Levine MS, Schmauss C, Zakharenko SS, Zablow L, and Sulzer D (2004). Heterosynaptic dopamine neurotransmission selects sets of corticostriatal terminals. Neuron 42, 653–663. [PubMed: 15157425]

Bellocchio L, Lafenetre P, Cannich A, Cota D, Puente N, Grandes P, Chaouloff F, Piazza PV, and Marsicano G (2010). Bimodal control of stimulated food intake by the endocannabinoid system. Nat Neurosci 13, 281–283. [PubMed: 20139974]

Berman SM, Kuczenski R, McCracken JT, and London ED (2009). Potential adverse effects of amphetamine treatment on brain and behavior: a review. Mol Psychiatry 14, 123–142. [PubMed: 18698321]

Blazquez C, Chiarlone A, Sagredo O, Aguado T, Pazos MR, Resel E, Palazuelos J, Julien B, Salazar M, Borner C, et al. (2011). Loss of striatal type 1 cannabinoid receptors is a key pathogenic factor in Huntington's disease. Brain 134, 119–136. [PubMed: 20929960]

Bourin M, and Hascoët M (2003). The mouse light/dark box test. European journal of pharmacology 463, 55–65. [PubMed: 12600702]

Busquets-Garcia A, Bains J, and Marsicano G (2018). CB 1 receptor signaling in the brain: extracting specificity from ubiquity. Neuropsychopharmacology 43, 4–20. [PubMed: 28862250]

Corbillé A-G, Valjent E, Marsicano G, Ledent C, Lutz B, Hervé D, and Girault J-A (2007). Role of cannabinoid type 1 receptors in locomotor activity and striatal signaling in response to psychostimulants. Journal of Neuroscience 27, 6937–6947. [PubMed: 17596442]

Costa RM, Cohen D, and Nicolelis MAL (2004). Differential Corticostriatal Plasticity during Fast and Slow Motor Skill Learning in Mice. In Current Biology, pp. 1124–1134. [PubMed: 15242609]

Covey DP, Mateo Y, Sulzer D, Cheer JF, and Lovinger DM (2017). Endocannabinoid modulation of dopamine neurotransmission. Neuropharmacology 124, 52–61. [PubMed: 28450060]

Davis MI, Crittenden JR, Feng AY, Kupferschmidt DA, Naydenov A, Stella N, Graybiel AM, and Lovinger DM (2018). The cannabinoid-1 receptor is abundantly expressed in striatal striosomes and striosome-dendron bouquets of the substantia nigra. PLoS One 13, e0191436. [PubMed: 29466446]

De Giacomo V, Ruehle S, Lutz B, Häring M, and Remmers F (2020a). Cell type-specific genetic reconstitution of CB1 receptor subsets to assess their role in exploratory behaviour, sociability and memory. European Journal of Neuroscience.

De Giacomo V, Ruehle S, Lutz B, Häring M, and Remmers F (2020b). Differential glutamatergic and GABAergic contributions to the tetrad effects of Δ9-tetrahydrocannabinol revealed by cell-type-specific reconstitution of the CB1 receptor. Neuropharmacology 179, 108287. [PubMed: 32860777]

Dobbs LK, Kaplan AR, Lemos JC, Matsui A, Rubinstein M, and Alvarez VA (2016). Dopamine regulation of lateral inhibition between striatal neurons gates the stimulant actions of cocaine. Neuron 90, 1100–1113. [PubMed: 27181061]

Freiman I, Anton A, Monyer H, Urbanski MJ, and Szabo B (2006). Analysis of the effects of cannabinoids on identified synaptic connections in the caudate-putamen by paired recordings in transgenic mice. The Journal of physiology 575, 789–806. [PubMed: 16825300]

Glass M, Dragunow M, and Faull RLM (1997). Cannabinoid receptors in the human brain: a detailed anatomical and quantitative autoradiographic study in the fetal, neonatal and adult human brain. Neuroscience 77, 299–318. [PubMed: 9472392]

Gremel CM, Chancey JH, Atwood BK, Luo G, Neve R, Ramakrishnan C, Deisseroth K, Lovinger DM, and Costa RM (2016). Endocannabinoid modulation of orbitostriatal circuits gates habit formation. Neuron 90, 1312–1324. [PubMed: 27238866]

Gremel CM, and Costa RM (2013). Orbitofrontal and striatal circuits dynamically encode the shift between goal-directed and habitual actions. Nature communications 4, 1–12.

Han X, He Y, Bi G-H, Zhang H-Y, Song R, Liu Q-R, Egan JM, Gardner EL, Li J, and Xi Z-X (2017). CB1 receptor activation on VgluT2-expressing glutamatergic neurons underlies Δ 9-tetrahydrocannabinol (Δ 9-THC)-induced aversive effects in mice. Scientific reports 7, 1–15. [PubMed: 28127051]

Häring M, Kaiser N, Monory K, and Lutz B (2011). Circuit specific functions of cannabinoid CB1 receptor in the balance of investigatory drive and exploration. PloS one 6, e26617. [PubMed: 22069458]

Hilário MR, Clouse E, Yin HH, and Costa RM (2007). Endocannabinoid signaling is critical for habit formation. Frontiers in integrative neuroscience 1, 6. [PubMed: 18958234]

Hoffman AF, and Lupica CR (2001). Direct actions of cannabinoids on synaptic transmission in the nucleus accumbens: a comparison with opioids. Journal of neurophysiology 85, 72–83. [PubMed: 11152707]

Hohmann AG, and Herkenham M (2000). Localization of cannabinoid CB1 receptor mRNA in neuronal subpopulations of rat striatum: A double-label in situ hybridization study. Synapse 37, 71–80. [PubMed: 10842353]

Hu SS-J, and Mackie K (2015). Distribution of the endocannabinoid system in the central nervous system. Endocannabinoids, 59–93.

Jang W-J, Son T, Song S-H, Ryu IS, Lee S, and Jeong C-H (2020). Transcriptional Profiling of Whisker Follicles and of the Striatum in Methamphetamine Self-Administered Rats. International journal of molecular sciences 21, 8856.

Kano M, Ohno-Shosaku T, Hashimotodani Y, Uchigashima M, and Watanabe M (2009). Endocannabinoid-mediated control of synaptic transmission. Physiol Rev 89, 309–380. [PubMed: 19126760]

Kreitzer AC, and Malenka RC (2005). Dopamine modulation of state-dependent endocannabinoid release and long-term depression in the striatum. J Neurosci 25, 10537–10545. [PubMed: 16280591]

Lafenetre P, Chaouloff F, and Marsicano G (2009). Bidirectional regulation of novelty-induced behavioral inhibition by the endocannabinoid system. Neuropharmacology 57, 715–721. [PubMed: 19607846]

Luo J, Kaplitt MG, Fitzsimons HL, Zuzga DS, Liu Y, Oshinsky ML, and During MJ (2002). Subthalamic GAD gene therapy in a Parkinson's disease rat model. Science 298, 425–429. [PubMed: 12376704]

Lutz B (2020). Neurobiology of cannabinoid receptor signaling. Dialogues in Clinical Neuroscience 22, 207. [PubMed: 33162764]

Maccarrone M, Guzmán M, Mackie K, Doherty P, and Harkany T (2014). Programming of neural cells by (endo) cannabinoids: from physiological rules to emerging therapies. Nature Reviews Neuroscience 15, 786–801. [PubMed: 25409697]

Marcellino D, Carriba P, Filip M, Borgkvist A, Frankowska M, Bellido I, Tanganelli S, Muller CE, Fisone G, Lluis C, et al. (2008). Antagonistic cannabinoid CB1/dopamine D2 receptor interactions in striatal CB1/D2 heteromers. A combined neurochemical and behavioral analysis. Neuropharmacology 54, 815–823. [PubMed: 18262573]

Marsicano G, Wotjak CT, Azad SC, Bisogno T, Rammes G, Cascio MG, Hermann H, Tang J, Hofmann C, Zieglgänsberger W, et al. (2002). The endogenous cannabinoid system controls extinction of aversive memories. Nature 418, 530–534. [PubMed: 12152079]

Massart R, Guilloux JP, Mignon V, Sokoloff P, and Diaz J (2009). Striatal GPR88 expression is confined to the whole projection neuron population and is regulated by dopaminergic and glutamatergic afferents. Eur J Neurosci 30, 397–414. [PubMed: 19656174]

Mathur BN, Tanahira C, Tamamaki N, and Lovinger DM (2013). Voltage drives diverse endocannabinoid signals to mediate striatal microcircuit-specific plasticity. Nature neuroscience 16, 1275–1283. [PubMed: 23892554]

Matyas F, Yanovsky Y, Mackie K, Kelsch W, Misgeld U, and Freund T (2006). Subcellular localization of type 1 cannabinoid receptors in the rat basal ganglia. Neuroscience 137, 337–361. [PubMed: 16289348]

Metna-Laurent M, Mondésir M, Grel A, Vallée M, and Piazza PV (2017). Cannabinoid-induced tetrad in mice. Current protocols in neuroscience 80, 9.59. 51–59.59. 10.

Monory K, Blaudzun H, Massa F, Kaiser N, Lemberger T, Schutz G, Wotjak CT, Lutz B, and Marsicano G (2007). Genetic dissection of behavioural and autonomic effects of Delta(9)-tetrahydrocannabinol in mice. PLoS Biol 5, e269. [PubMed: 17927447]

Naydenov AV, Sepers MD, Swinney K, Raymond LA, Palmiter RD, and Stella N (2014). Genetic rescue of CB1 receptors on medium spiny neurons prevents loss of excitatory striatal synapses but not motor impairment in HD mice. Neurobiol Dis 71, 140–150. [PubMed: 25134728]

Newcorn JH (2001). New treatments and approaches for attention deficit hyperactivity disorder. Current psychiatry reports 3, 87–91. [PubMed: 11276402]

Opiol H, de Zavalia N, Delorme T, Solis P, Rutherford S, Shalev U, and Amir S (2017). Exploring the role of locomotor sensitization in the circadian food entrainment pathway. PloS one 12, e0174113. [PubMed: 28301599]

Parsons LH, and Hurd YL (2015). Endocannabinoid signalling in reward and addiction. Nature Reviews Neuroscience 16, 579–594. [PubMed: 26373473]

Peak J, Hart G, and Balleine BW (2019). From learning to action: the integration of dorsal striatal input and output pathways in instrumental conditioning. European Journal of Neuroscience 49, 658–671. [PubMed: 29791051]

Pennartz CM, Groenewegen HJ, and Lopes da Silva FH (1994). The nucleus accumbens as a complex of functionally distinct neuronal ensembles: an integration of behavioural, electrophysiological and anatomical data. Prog Neurobiol 42, 719–761. [PubMed: 7938546]

Pham J, Cabrera SM, Sanchis-Segura C, and Wood MA (2009). Automated scoring of fear-related behavior using EthoVision software. Journal of neuroscience methods 178, 323–326. [PubMed: 19150629]

Pickel VM, Chan J, Kearn CS, and Mackie K (2006). Targeting dopamine D2 and cannabinoid-1 (CB1) receptors in rat nucleus accumbens. The Journal of comparative neurology 495, 299–313. [PubMed: 16440297]

Quintana A, Sanz E, Wang W, Storey GP, Güler AD, Wanat MJ, Roller BA, La Torre A, Amieux PS, and McKnight GS (2012). Lack of GPR88 enhances medium spiny neuron activity and alters motor-and cue-dependent behaviors. Nature neuroscience 15, 1547–1555. [PubMed: 23064379]

Reith ME, and Gnegy ME (2019). Molecular Mechanisms of Amphetamines.

Remmers F, Lange MD, Hamann M, Ruehle S, Pape H-C, and Lutz B (2017). Addressing sufficiency of the CB1 receptor for endocannabinoid-mediated functions through conditional genetic rescue in forebrain GABAergic neurons. Brain Structure and Function 222, 3431–3452. [PubMed: 28393261]

Richetto J, Feldon J, Riva MA, and Meyer U (2013). Comparison of the long-term consequences of withdrawal from repeated amphetamine exposure in adolescence and adulthood on information processing and locomotor sensitization in mice. Eur Neuropsychopharmacol 23, 160–170. [PubMed: 22609316]

Robinson TE, and Becker JB (1986). Enduring changes in brain and behavior produced by chronic amphetamine administration: a review and evaluation of animal models of amphetamine psychosis. Brain Res 396, 157–198. [PubMed: 3527341]

Ruehle S, Remmers F, Romo-Parra H, Massa F, Wickert M, Wörtge S, Häring M, Kaiser N, Marsicano G, and Pape H-C (2013). Cannabinoid CB1 receptor in dorsal telencephalic glutamatergic neurons: distinctive sufficiency for hippocampus-dependent and amygdala-dependent synaptic and behavioral functions. Journal of Neuroscience 33, 10264–10277. [PubMed: 23785142]

Sarris J, Sinclair J, Karamacoska D, Davidson M, and Firth J (2020). Medicinal cannabis for psychiatric disorders: a clinically-focused systematic review. BMC psychiatry 20, 1–14. [PubMed: 31898506]

Soria-Gomez E, Zottola ACP, Mariani Y, Desprez T, Barresi M, Bonilla-del Río I, Muguruza C, Le Bon-Jego M, Julio-Kalajzić F, and Flynn R (2021). Subcellular specificity of cannabinoid effects in striatonigral circuits. Neuron.

Steele AD, Jackson WS, King OD, and Lindquist S (2007). The power of automated high-resolution behavior analysis revealed by its application to mouse models of Huntington's and prion diseases. Proc Natl Acad Sci U S A 104, 1983–1988. [PubMed: 17261803]

Steindel F, Lerner R, Häring M, Ruehle S, Marsicano G, Lutz B, and Monory K (2013). Neuron-type specific cannabinoid-mediated G protein signalling in mouse hippocampus. Journal of neurochemistry 124, 795–807. [PubMed: 23289830]

Sulzer D, Sonders MS, Poulsen NW, and Galli A (2005). Mechanisms of neurotransmitter release by amphetamines: a review. Prog Neurobiol 75, 406–433. [PubMed: 15955613]

Szabo B, Dörner L, Pfreundtner C, Nörenberg W, and Starke K (1998). Inhibition of GABAergic inhibitory postsynaptic currents by cannabinoids in rat corpus striatum. Neuroscience 85, 395–403. [PubMed: 9622239]

Tsou K, Brown S, Sanudo-Pena MC, Mackie K, and Walker JM (1998). Immunohistochemical distribution of cannabinoid CB1 receptors in the rat central nervous system. Neuroscience 83, 393–411. [PubMed: 9460749]

Turner BD, Smith NK, Manz KM, Chang BT, Delpire E, Grueter CA, and Grueter BA (2021). Cannabinoid type 1 receptors in A2a neurons contribute to cocaine-environment association. Psychopharmacology, 1–11.

Uchigashima M, Narushima M, Fukaya M, Katona I, Kano M, and Watanabe M (2007). Subcellular arrangement of molecules for 2-arachidonoyl-glycerol-mediated retrograde signaling and its physiological contribution to synaptic modulation in the striatum. J Neurosci 27, 3663–3676. [PubMed: 17409230]

Vezina P, and Stewart J (1989). The effect of dopamine receptor blockade on the development of sensitization to the locomotor activating effects of amphetamine and morphine. Brain Res 499, 108–120. [PubMed: 2679971]

Walker FO (2007). Huntington's disease. In Lancet (Elsevier), pp. 218–228.

Wang W, Darvas M, Storey GP, Bamford IJ, Gibbs JT, Palmiter RD, and Bamford NS (2013). Acetylcholine encodes long-lasting presynaptic plasticity at glutamatergic synapses in the dorsal striatum after repeated amphetamine exposure. J Neurosci 33, 10405–10426. [PubMed: 23785153]

Wang W, Dever D, Lowe J, Storey GP, Bhansali A, Eck EK, Nitulescu I, Weimer J, and Bamford NS (2012). Regulation of prefrontal excitatory neurotransmission by dopamine in the nucleus accumbens core. J Physiol 590, 3743–3769. [PubMed: 22586226]

Wiley JL, and Martin BR (2003). Cannabinoid pharmacological properties common to other centrally acting drugs. European journal of pharmacology 471, 185–193. [PubMed: 12826237]

Yin HH, Knowlton BJ, and Balleine BW (2006). Inactivation of dorsolateral striatum enhances sensitivity to changes in the action–outcome contingency in instrumental conditioning. Behavioural brain research 166, 189–196. [PubMed: 16153716]

Yin HH, and Lovinger DM (2006). Frequency-specific and D2 receptor-mediated inhibition of glutamate release by retrograde endocannabinoid signaling. Proc Nat Acad Sci 103, 8251–8256. [PubMed: 16698932]

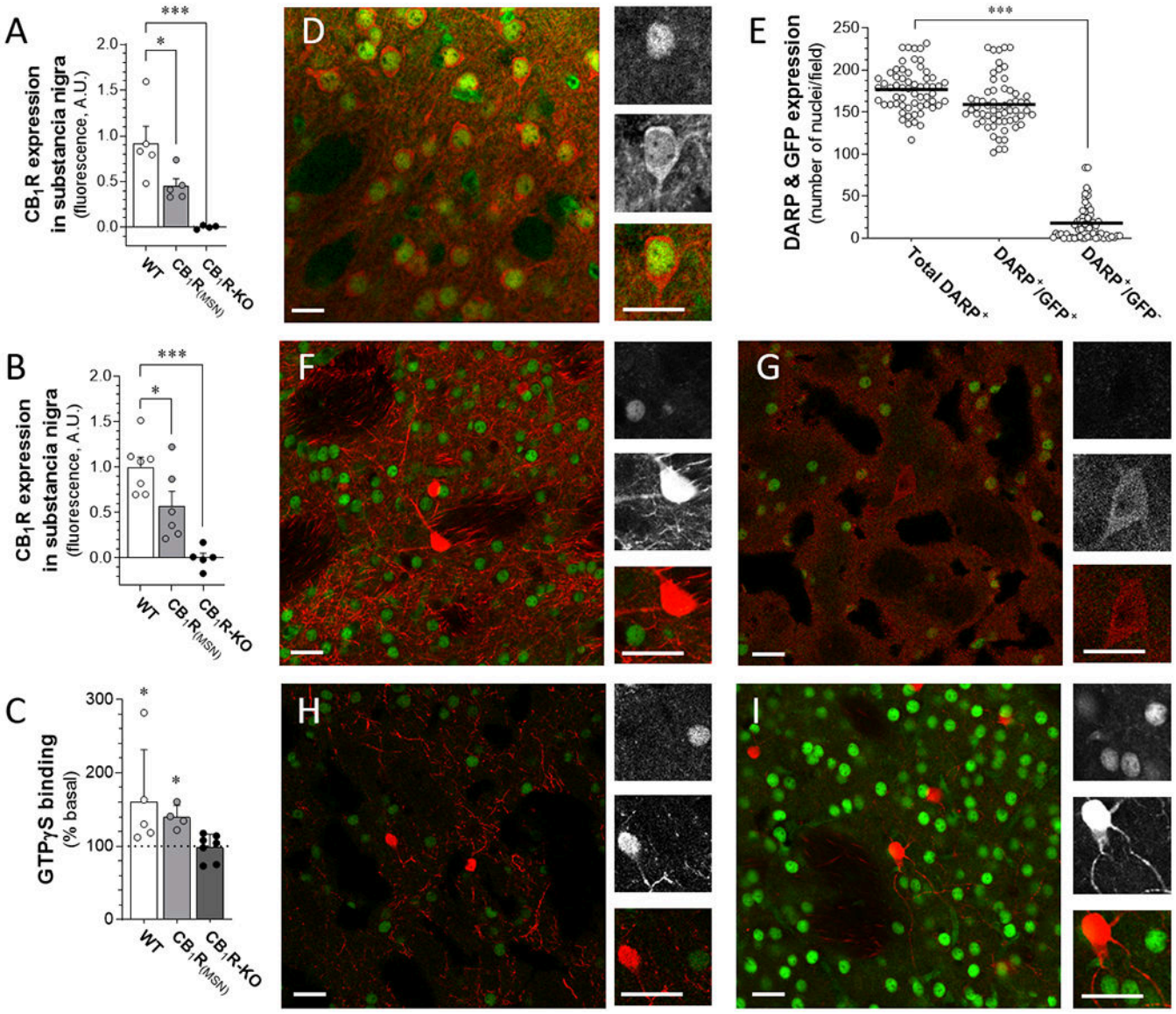

Figure 1: Validation of CB_1R expression and functionality in medium spiny neurons of $CB_1R_{(MSN)}$ mice.

Expression of flox-stop (fs)-derived CB_1R, eGFP and interneuron markers in striatum measured by sq-IHC, and functionality of fs-CB_1-derived CB_1R measured in substantia nigra reticulata (SNr) by measuring GTPγS binding. **A.** Expression of fs-CB_1-derived CB_1R in SNr (Data are mean ± S.E.M. of n mice: WT n=5, $CB_1R_{(MSN)}$ n=5 and CB_1R KO n=4). **B.** Expression of fs-CB_1-derived CB_1R in the globus pallidus (Data are mean S.E.M. of n mice: WT n=7, $CB_1R_{(MSN)}$ n=5 and CB_1R KO n=6). (A-B) *p<0.05 and ***p<0.001 significantly different from WT using ordinary one-way ANOVA analyses (Tukey's multiple comparisons test). **C.** Functional G protein-coupling of fs-CB_1-derived CB_1R was measured by changes in GTPγS binding in response to CP55940 tested at its EC_{80} (140 nM). Results are mean ± S.E.M. of n mice. *p<0.05 significantly different from vehicle treated samples using ordinary one-way ANOVA analyses (Tukey's multiple comparisons test). **(D-I)** Fraction of striatal cells that express EGFP (green, expressed from

the same transcript by using the internal ribosome entry sequence) and either marker of GABAergic interneurons (red): (D) DARPP32 (medium spiny neurons), (F) calretinin, (G) neuropeptide Y, (H) parvalbumin, or (I) choline acetyltransferase. Scale bar = 25 μm. (E) Number of striatal cells labelled by DARPP and/or EGFP were analyzed by an automated scoring system in ImageJ to count co-labeled or singly labeled somas in striatal sections. Results show single cells (dots) labelled in n = 3 striatal sections from $CB_1R_{(MSN)}$ mice. ***$p<0.001$ significantly different from total $DARPP^+$ using ordinary one-way ANOVA analyses (Tukey's multiple comparisons test).

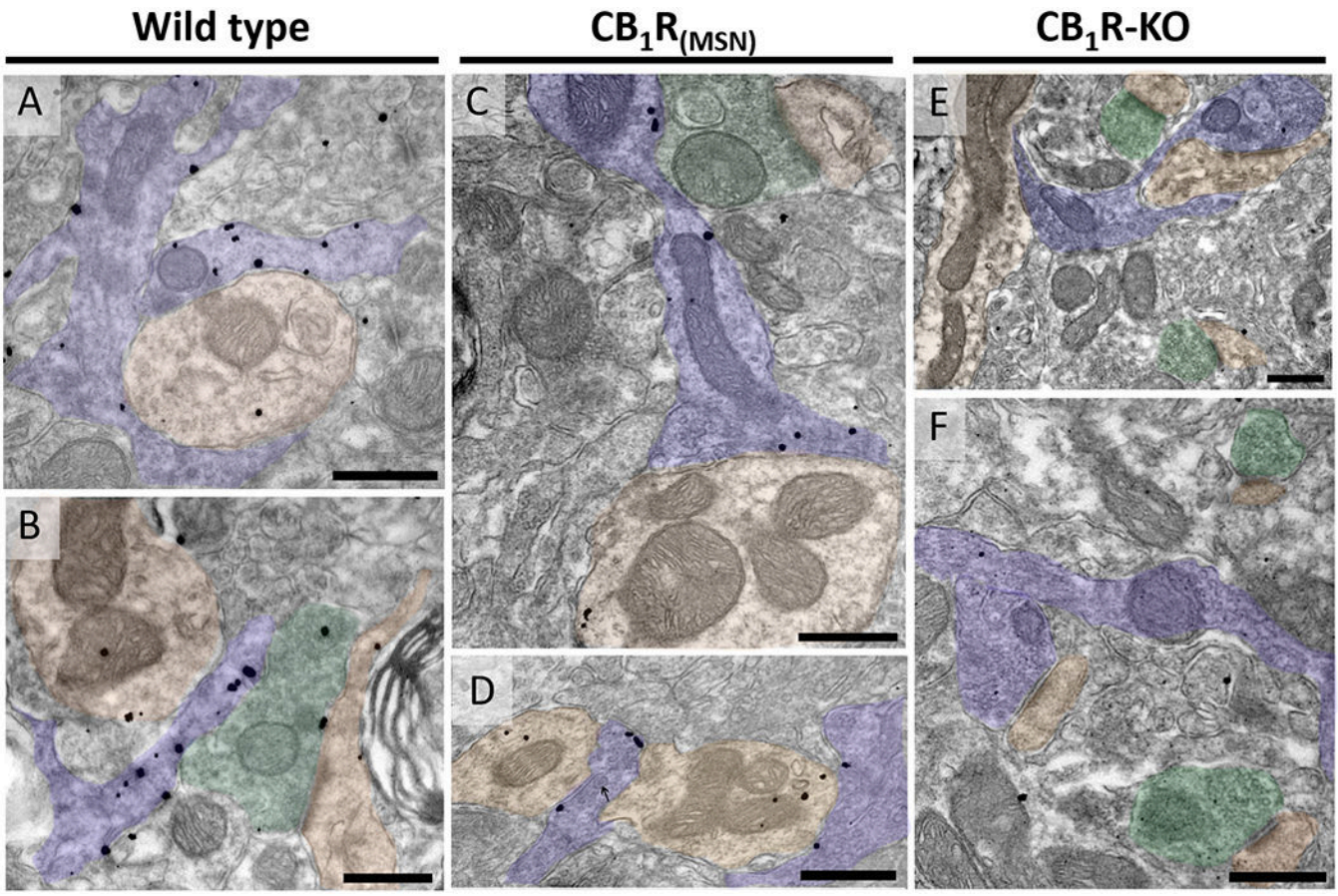

Figure 2: Subcellular CB_1R expression in medium spiny neurons of $CB_1R_{(MSN)}$ mice.
Subcellular expression of CB_1R in striatum of WT, $CB_1R_{(MSN)}$ and CB_1R KO mice using a pre-embedding immunogold method and electron microscopy visualization. **A-D.** CB_1R immunoparticles localize in terminals (blue shading) forming symmetric (inhibitory) synapses with dendrites (orange shading) in WT (A-B) and $CB_1R_{(MSN)}$ (C-D), and in terminals (green shading) making asymmetric (excitatory) synapses with dendritic spines (orange shading) in WT (B). Note the absence of CB_1R labeling in an excitatory terminal (green shading in C) and the presence of a dense core vesicle in a typical MSN collateral terminal with CB_1R particles over extrasynaptic membranes (arrow in D) in $CB_1R_{(MSN)}$ (C-D). **E-F.** Background level is negligible in CB_1R KO. Scale bar = 0.5 μm.

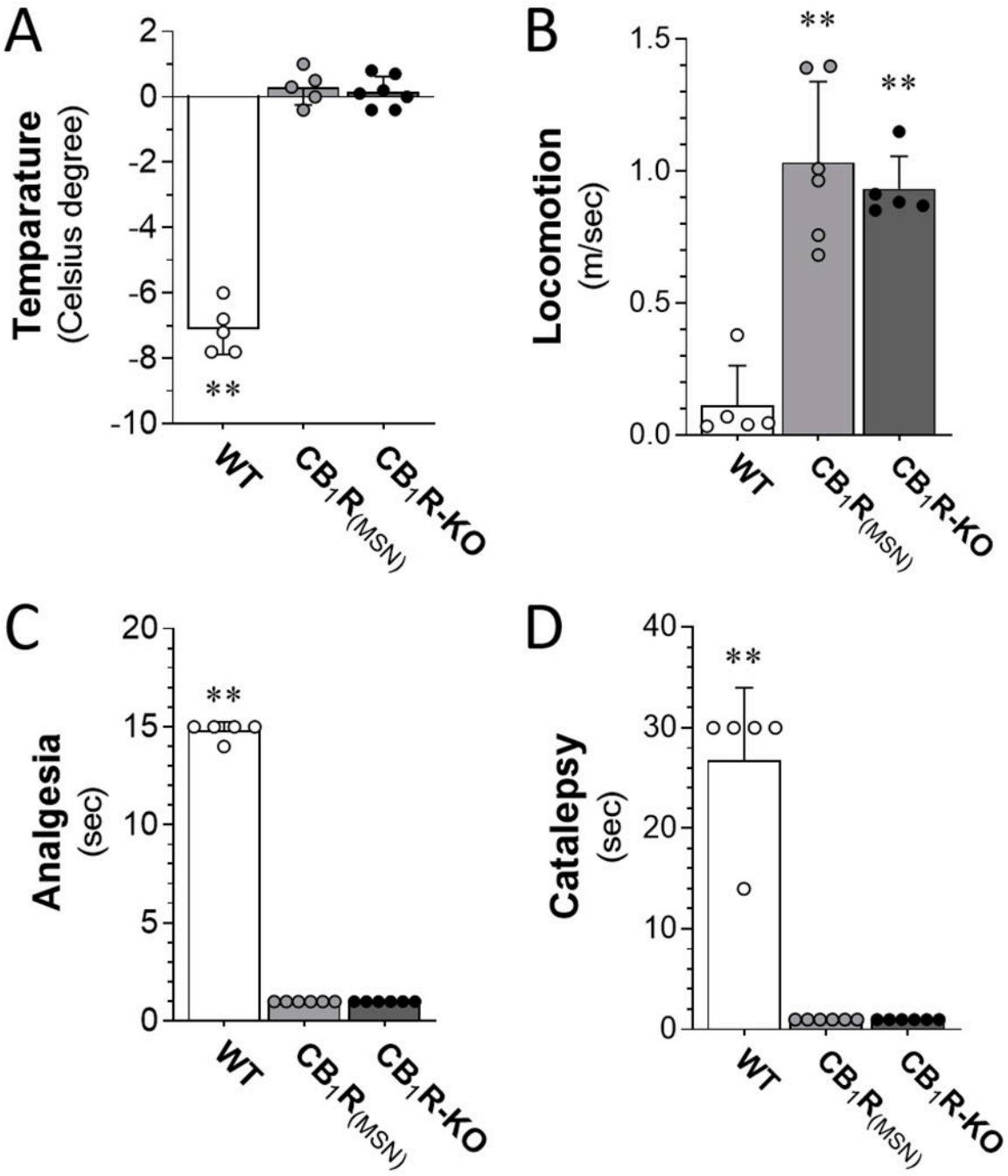

Figure 3: Absence of cannabimimetic tetrad behavioral responses in $CB_1R_{(MSN)}$ mice.

Cannabimimetic behaviors (i.e., tetrad response) measured in mice of each genotype treated with CP55,940 (3 mg/kg, i.p.). **A.** CP55,940 induced significant decrease in body temperature in WT mice, and not in $CB_1R_{(MSN)}$ and CB_1R KO mice as measured by a rectal thermometer (Celsius degree). **B.** CP55,940 induced significant decrease in locomotion in WT mice, and not in $CB_1R_{(MSN)}$ and CB_1R KO mice as measured in an open field (m/s). **C.** CP55,940 induced a significant analgesia in WT mice, and not in $CB_1R_{(MSN)}$ and CB_1R KO mice as measured by the latency (s) to withdraw the tail from 52.5 ± 0.5 °C water. **D.**

CP55,940 induced significant catalepsy in WT mice, and not in $CB_1R_{(MSN)}$ and CB_1R KO mice as measured by the latency to withdraw from a standing horizontal bar. Data are mean ± S.E.M. of n = 5 mice of each genotype. **p<0.01 when significantly different from control behavior response (vehicle, i.p. injection, zero value in each graph) using two-way ANOVA analyses.

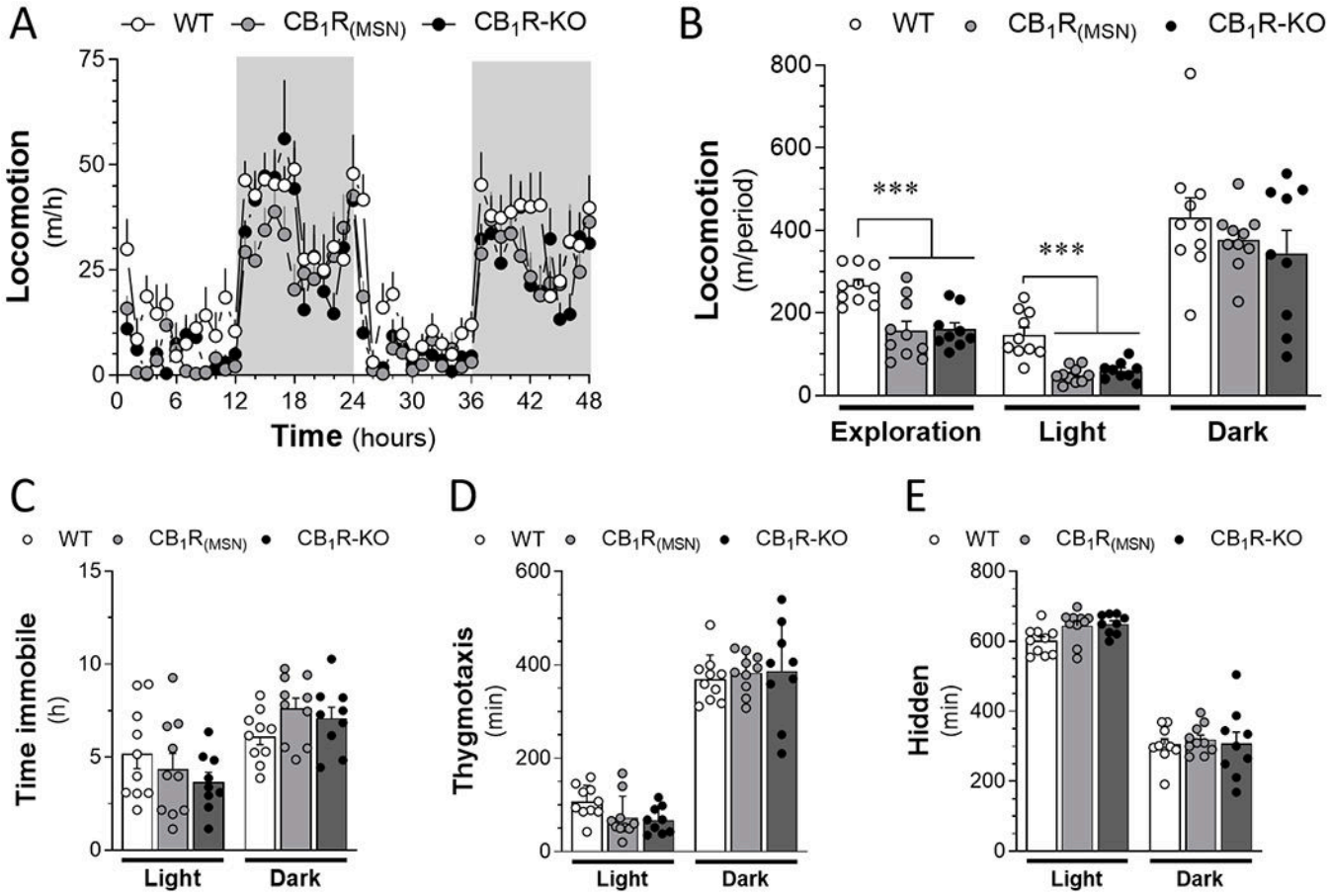

Figure 4: Spontaneous locomotion of $CB_1R_{(MSN)}$ mice.

The spontaneous locomotion measured in Phenotyper home-cages monitoring system in mice of each genotype over 48 h. **A.** Spontaneous locomotion (meters/h) measured in 2 h bins over 48 h (12 h light and dark cycles; beginning at 24 h and ending at 72 h after housing). **B.** Average spontaneous locomotion (m/period) during exploration (initial two hours of housing in the Phenotyper chambers), light cycles (combined 12 h light), or dark cycles (combined 12 h light). **C-E.** Time spent immobile (C), close to the edge of the home chamber (Thigmotaxis, D) and in the hidden area of the home chamber (E) during light cycles (combined 12 h light) and dark cycles (combined 12 h light). Data are mean ± S.E.M. of WT (n = 10), $CB_1R_{(MSN)}$ (n = 11) and $CB_1R^{-/-}$ mice (n = 8). ***p<0.001 significantly different using multiple comparison two-way ANOVA analyses (Tukey's multiple comparisons test).

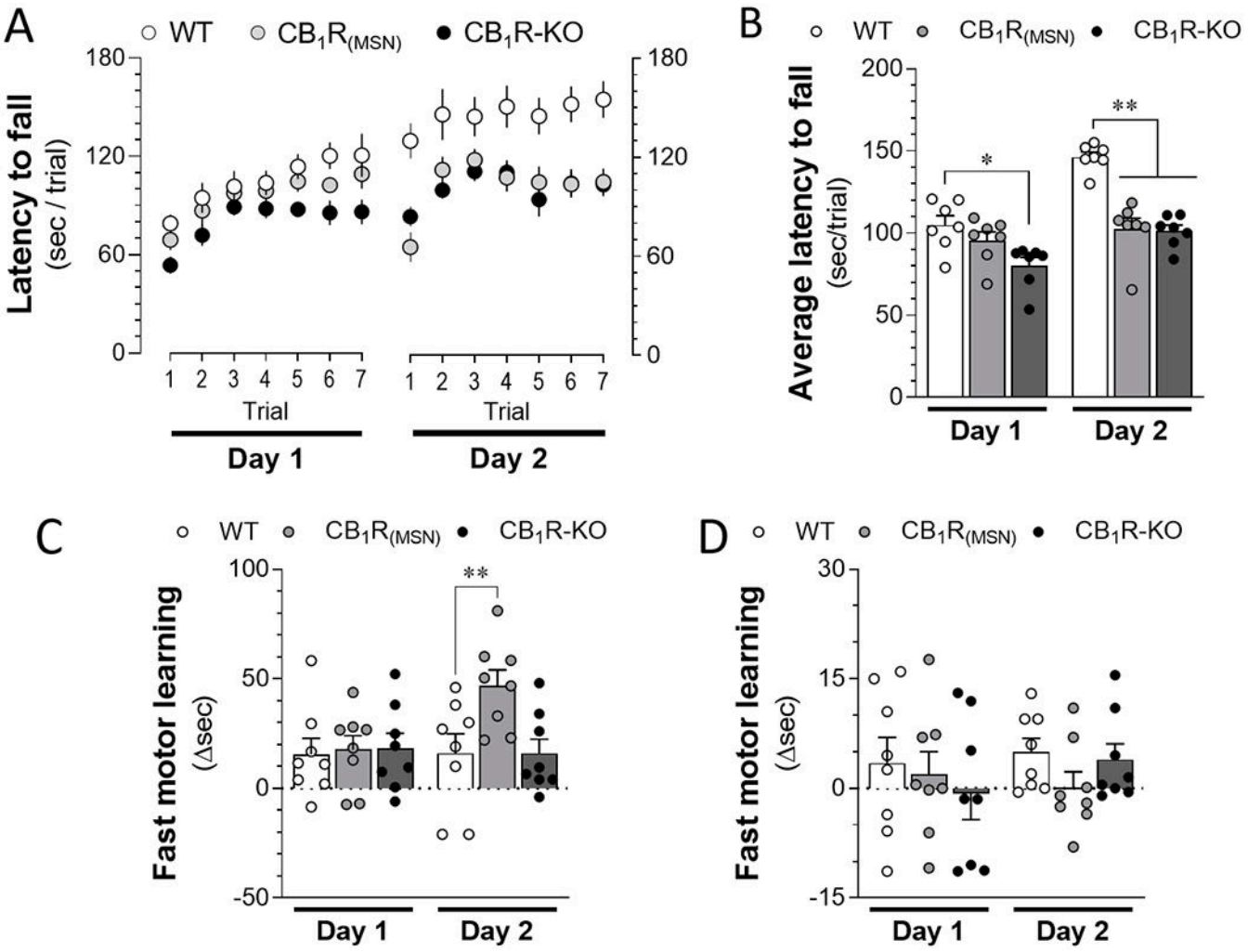

Figure 5: Motor coordination of $CB_1R_{(MSN)}$ mice.

Motor coordination were measured on Rotarod apparatus in mice of each genotype. **A.** Motor coordination measured by the latency to fall from the Rotarod (sec/trial) over 7 trials and 2 days. **B.** Average latency to fall (sec/trial) measured each day. **C.** Fast motor learning measured during the initial 4 trials of days 1 and 2 of testing. **D.** Slow motor learning measured by the sum of improvement in performance across all trials. Results are mean ± S.E.M. from n = 8 mice of each genotype. *p<0.05 and **p<0.01 significantly different using multiple comparison two-way ANOVA analyses (Tukey's multiple comparisons test).

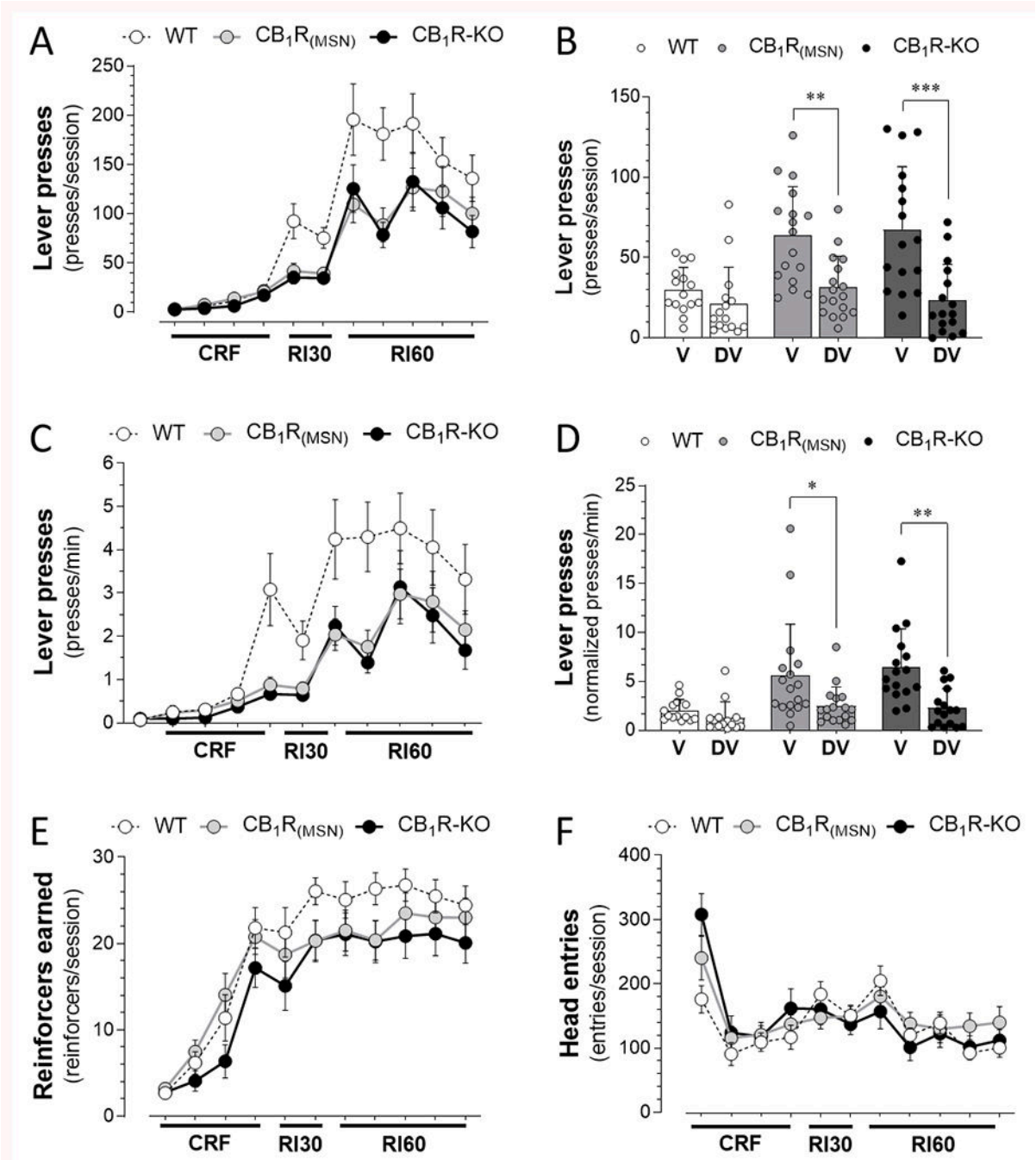

Figure 6: Habit formation of $CB_1R_{(MSN)}$ mice.

Habit formation measured using lever press revaluation in mice of each genotype. **A.** Number of lever presses (presses/session) measured during continuous reinforcement (CRF) schedule and random interval (RI) reinforcement of 30 sec (RI30) schedule and of 60 sec (RI60). **B.** Average lever presses (presses/session) measured on the valued (V) and devalued days (DV). **P<0.01, and **P<0.01 significantly different using multiple comparison two-way ANOVA analyses (Tukey's multiple comparisons test). **C.** Rate of lever presses (presses/min) measured during CRF schedule, RI30 and RI60. **D.** Average

rate of lever presses (normalized/presses/min) measured for the V and DV days. *P<0.05, and **P<0.01 significantly different using multiple comparison two-way ANOVA analyses (Tukey's multiple comparisons test). **E.** Reinforcers earned (reinforcers/session; max set at 30 reinforcers per session) during CRF schedule, RI30 and RI60. **F.** Number of head entries (entry/session) measured during CRF schedule, RI30 and RI60. No significant difference using two-way ANOVA analyses. All results are mean ± S.E.M. from WT (n = 14), $CB_1R_{(MSN)}$ (n = 17) and CB_1R KO mice (n = 16).

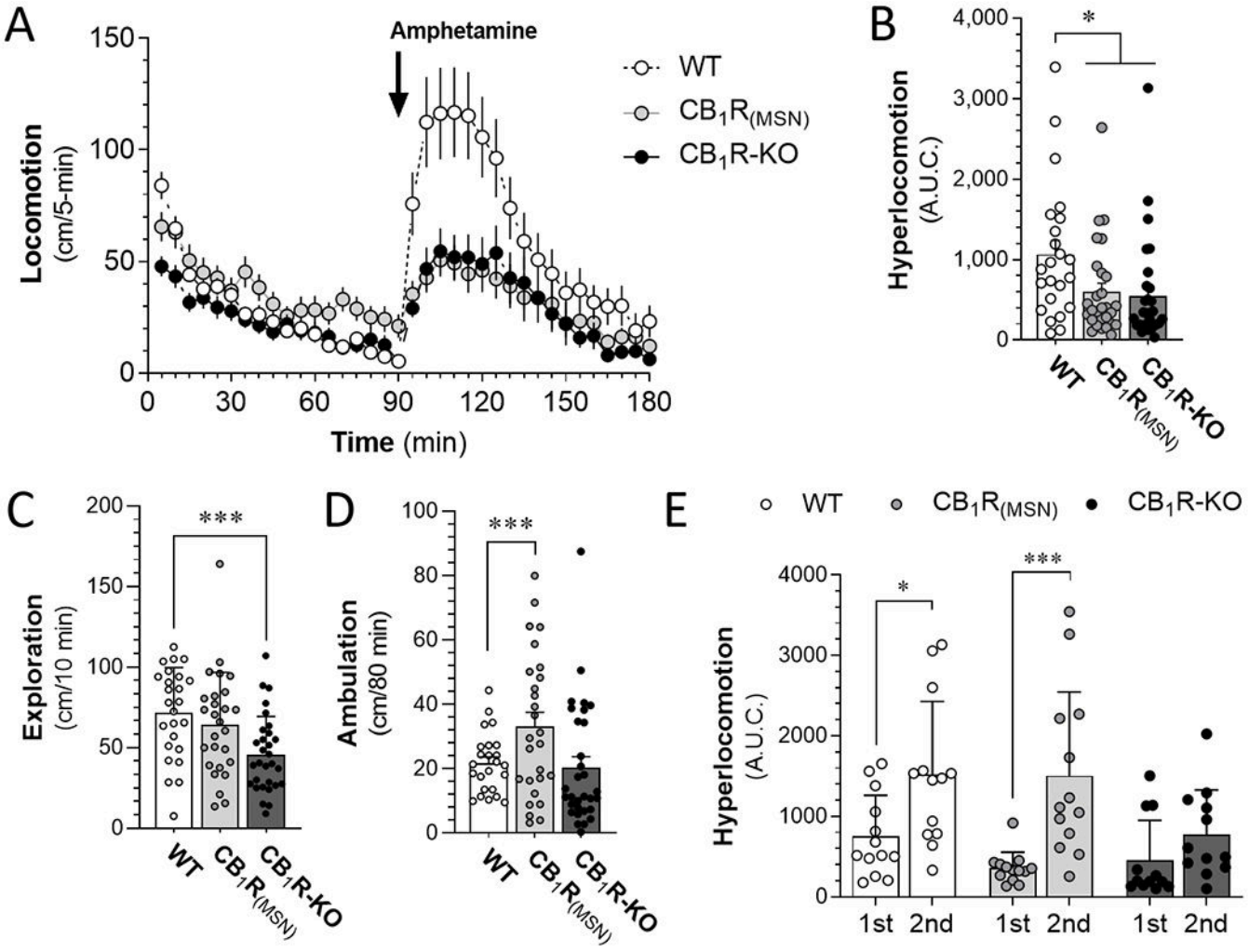

Figure 7: CB_1R expression in medium spiny neurons are sufficient to rescue amphetamine sensitization and not involved in acute amphetamine triggered hyperlocomotion.

Acute amphetamine hyperlocomotion and its sensitization resulting from a second amphetamine injections (2 mg/kg) were measured by videorecording of locomotion in an open field in mice of each genotype. **A.** Open filed ambulation (cm/min) before and after amphetamine injection (arrow). **B-D.** Total amphetamine induced hyperlocomotion (B, locomotion 90 min following amphetamine treatment, AUC in m), spontaneous locomotion during initial exploration (C, initial 10 min, m), spontaneous ambulation following initial exploration (D, 10-90 min following placement in open field, cm). Results are mean ± S.E.M. of n mice: WT (n = 26), $CB_1R_{(MSN)}$ (n = 27) and CB_1R KO mice (n = 31). *p<0.05 and ***p<0.001 significantly different using multiple comparison two-way ANOVA analyses (Tukey's multiple comparisons test). **E.** Average amphetamine induced hyperlocomotion (1^{st} Amph) and sensitization (2^{nd} Amph) (locomotion 90 min following amphetamine treatment, AUC). Data are mean ± S.E.M. of WT (n=12), $CB_1R_{(MSN)}$ (n = 12) and CB_1R KO (n = 13) mice. *P<0.05, and ***P<0.001 significantly different using multiple comparison two-way ANOVA analyses (Tukey's multiple comparisons test).